METRICA
METRology Institutional CAtalog

ISTITUTO NAZIONALE DI RICERCA METROLOGICA
Repository Istituzionale

Josephson Traveling Wave Parametric Amplifier as Quantum Source of Entangled Photons for Microwave Quantum Radar Applications

Original
Josephson Traveling Wave Parametric Amplifier as Quantum Source of Entangled Photons for Microwave Quantum Radar Applications / Livreri, Patrizia; Galvano, Bernardo; Fasolo, Luca; Oberto, Luca; Enrico, Emanuele. - In: ELECTROMAGNETIC WAVES. - ISSN 1559-8985. - 179:(2024), pp. 113-124. [10.2528/pier24041705]

Availability:
This version is available at: 11696/81599 since: 2024-09-09T12:06:44Z

Publisher:
EMW PUBLISHING

Published
DOI:10.2528/pier24041705

Terms of use:

This article is made available under terms and conditions as specified in the corresponding bibliographic description in the repository

Publisher copyright

(Article begins on next page)

07 February 2025

(Received 17 April 2024, Accepted 25 July 2024, Scheduled 28 August 2024)

Josephson Traveling Wave Parametric Amplifier as Quantum Source of Entangled Photons for Microwave Quantum Radar Applications

Patrizia Livreri[1, 2, *], Bernardo Galvano[1, 2, 3], Luca Fasolo[3], Luca Oberto[3], and Emanuele Enrico[3]

[1] *University of Palermo, Department of Engineering, 90128, Palermo, Italy*
[2] *Consorzio Nazionale Interuniversitario per le Telecomunicazioni, Viale G.P. Usberti, 181/A, Parma, Italy*
[3] *Istituto Nazionale di Ricerca Metrologica — INRiM, strada delle Cacce, 91, 10135, Torino, Italy*

ABSTRACT: Josephson Traveling Wave Parametric Amplifier (JTWPA) has the potential to offer quantum limited noise and a large bandwidth. This amplifier is based on parametric amplification of microwaves traveling through a transmission line with embedded non-linear elements. In this paper, starting from the fabrication of the JTWPA, based on Quantum Electrodynamics (QEDs), operating as a non-classical quantum source for generating a signal-idler entangled state, its characterization in terms of scattering parameters is presented. The cryogenic and room temperature experimental results are discussed. The good performance of the JTWPA in terms of wide bandwidth and increased transmitted power makes it an ideal candidate for Microwave Quantum Radar (MQR) applications. Finally, the performance of an MQR based on the JTWPA developed at INRiM is reported, showing a radar maximum range equal to 82.2 m, which represents a greater value than previously published works.

1. INTRODUCTION

Quantum Radar concept began with the initial proposal of an interferometric quantum radar by Dowling [1] and evolved simultaneously through the work of Lloyd, who introduced the idea of Quantum Illumination (QI) [2], well developed by other important research groups [3–7]. A radar is a remote sensing system developed to detect very low cross-radar section targets. Photonics and electronic quantum sensing systems exploit quantum advantage [2, 8–10]. Photonics quantum sensing technology has been largely proposed for its simplicity compared to electronics quantum sensing [11, 12]. Recently, the generation of quantum signals at microwaves has been proved [13–20], paving the way for microwave quantum radars (MQRs). Quantum Illumination exploits the phenomenon of entanglement, a condition in which two or more physical systems are interconnected in such a way that the overall quantum state is a superposition of their individual states, to make a precise distinction between the signal and background noise. To illustrate, a typical quantum illumination procedure is characterized by the generation of two entangled signals, one of which is sent towards a target while the other is used for performing a simultaneous comparison measurement with the returned signal received. This process of comparing the two signals allows us to identify whether the received signal is indeed a signal coming back or just noise.

The original idea of QI was not specifically aimed at the development of quantum radars, and those who had the intuition to apply such a protocol to realize radars encountered various problems immediately. Indeed, this technique presents significant challenges, particularly the difficulty of performing simultaneous and joint measurements on two entangled pulses without precise preexisting knowledge of the distance to the target. This complication makes the original QI protocol impractical for traditional radar applications.

In 2019, Luong et al. presented the first microwave quantum radar that operated with microwave entangled photons [10]. The proposed system is based on a Josephson Parametric Amplifier (JPA) as a quantum source generating radio frequency (RF) entangled signal-idler pairs at 7.5376 GHz and 6.1445 GHz, respectively. The transmitted signal, scattered from the target is extracted from the background noise owing to the correlation between the idler and the signal. However, the JPA exploited in MQR is limited in terms of operating bandwidth owing to its high-quality factor resonator. The narrow bandwidth B limits the transmitted power P, because $P = EB$ for one photon per mode with energy E. Moreover, the number of interrogating pulses, given by $M = TB$ with T being the time duration of the illumination [21, 22], is limited. Consequently, the JPA, with a maximum dynamic bandwidth equal to a few MHz, is expected to be useful only for very short range (cm-range) MQR applications (see also the very recent demonstration of quantum advantage at ultracryogenic temperatures by Assouly et al. [23], employing a JPA). To overcome these limitations, superconducting technology has approached the so-called Josephson Traveling Wave Parametric Amplifiers (JTWPAs) [24, 25].

Over the years, several proposals have been made to overcome these issues. One of the particular interests is the Quan-

* Corresponding author: Patrizia Livreri (patrizia.livreri@unipa.it).

tum Two-Mode Squeezing Radar (QTMS radar) [26–28]. This technique exploits a specific type of continuous-variable quantum entanglement known as Two-Mode Squeezed Vacuum (TMSV). Similar to QI, this technique is based on the generation of two entangled signals where one is sent to free space, and the other is measured. To distinguish an actual signal from noise, the metric of interest is the covariance matrix, which allows the quantification of the correlation of a pair of signals. These matrices are constructed with the distributions of the signals in the phase and quadrature (I-Q) planes [29]. The covariance matrix contains all the information on the correlation between states, allowing them to be identified as entangled or not.

In this study, the characterization of scattering parameters of JTWPAs, fabricated at INRiM, operating as a non-classical quantum source in an ultra-cryogenic environment, is reported. These results indicate that the JTWPAs perform well under real conditions, encouraging their practical applicability. Microwave entangled signal-idler signals in a TMSV state are exploited for microwave quantum radar applications. Compared with a JPA quantum technologies, JTWPAs provide a substantial leap forward with their broad operational bandwidth. The performance of a microwave quantum radar based on the developed JTWPA is evaluated, and a radar maximum range equal to 82.2 m is obtained. This is a notable improvement over traditional JPAs, which suffer from limited range and power output. The enhanced bandwidth and efficiency of JTWPAs mean that MQR systems can now have a longer range and more powerful performance, overcoming previous limitations, as given by the JPA.

The article is organized as follows. In Section 2, we briefly describe the quantum illumination protocol. In Section 3, the non-linearity of the JTWPA is discussed, and the relationships between the scattering parameter and gain are reported. Moreover, the squeezing produced by the devices of interest is addressed. Section 4 presents the preliminary experimental results. In Section 5, the performance of a microwave quantum radar using JTWPA as the quantum source is reported. Finally, conclusions are presented in Section 6.

2. QUANTUM ILLUMINATION PROTOCOL

Quantum illumination (QI) is a quantum remote sensing protocol in which shared entanglement between an electromagnetic (EM) mode (annihilation operator a_S, the signal) probing a target region and a second EM mode (annihilation operator a_I, the idler) stored locally in the emitting station is used to detect the presence of a remote target (see Fig. 1).

The quantum correlations of the transmitted state are exploited at the receiving station by means of proper joint measurement on the signal and idler modes. The peculiar aspect of QI is that quantum advantage manifests itself in the unexpected regime of low signal and large background thermal noise, in which the initial entanglement contained in the quantum state sent by the transmitter is rapidly destroyed.

The problem is modeled as a binary decision problem with two hypotheses, H_0 (target absent) and H_1 (target present) [2]. With absent target, the return mode arriving at the receiver (with annihilation operator a_R) is given by $a_R = a_B$, where

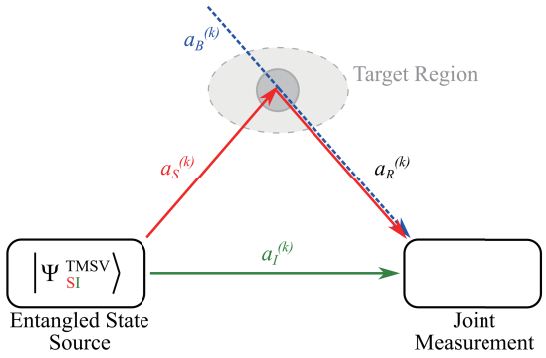

FIGURE 1. Schematic description of target detection via quantum illumination.

a_B describes a thermal background EM mode with $\langle a_B^\dagger a_B\rangle = N_B \gg 1$. In the presence of the target (H_1) instead, $a_R = \sqrt{\kappa}a_S + \sqrt{1-\kappa}a_B$, with $\kappa \ll 1$ the roundtrip sender-target-receiver transmissivity, and $\langle a_B^\dagger a_B\rangle = N_B/(1-\kappa)$, so that the mean noise photon number is equal under both hypotheses.

QI was first proposed and analyzed within a Bayesian decision approach [30], i.e., in which one aims to minimize the mean error probability $P_e = \lambda P_M + (1-\lambda)P_F$, where $P_M = \text{Prob}(H_0|H_1)$ is the miss probability; $P_F = \text{Prob}(H_1|H_0)$ is the false-alarm probability; and λ is the *a priori* probability for target presence, usually assumed to be equal to $1/2$. Ref. [22] shows that by choosing as the signal-idler state to be transmitted, a TMSV state

$$|\Psi\rangle_{SI} = \sum_{n=0}^{\infty} \sqrt{\frac{N_S^n}{(N_S+1)^{n+1}}}|n\rangle_S|n\rangle_I, \tag{1}$$

where $\langle a_S^\dagger a_S\rangle = \langle a_I^\dagger a_I\rangle = N_S$ and $\langle a_S a_I\rangle = \sqrt{N_S(N_S+1)}$ are the only nonzero first-order and second-order correlations. To achieve a satisfactory signal-to-noise ratio $SNR = M\kappa N_S/N_B$, it must hold that $M \gg 1$, and this allows us to reach the minimum value of P_e allowed by quantum mechanics, known as the Helstrom bound [31]. In particular, in the assumed working regime of low signal $N_S \ll 1$, and large background thermal noise $N_B \gg 1$. They showed that when $M \gg 1$,

$$P_e^{QI} \leq e^{-M\kappa N_S/N_B}/2. \tag{2}$$

Ref. [22] also determined the optimal classical binary decision strategy, that is, using only the *classical* states of the EM field: sending M identical coherent states of the signal mode with the same mean energy N_S, $|\sqrt{N_S}\rangle$ directly to the target. In the latter case they proved that in the limit of a large M

$$P_e^{CS} \leq e^{-M\kappa N_S/4N_B}/2, \tag{3}$$

implying that QI provides an improvement by a factor of 4 (i.e., 6 dB) in the error rate exponent compared with the best classical protocol with the same signal photon number N_S. We notice that in both cases it is $M = BT$, where M is the number of independent pulses emitted by the quantum source; T is the time duration of the illumination; and B is the bandwidth of the coherent source in the classical case, while it coincides with the

phase-matching bandwidth of the entangled signal-idler source in the QI case.

3. JOSEPHSON TRAVELING WAVE PARAMETRIC AMPLIFIER: SQUEEZED STATES VIA JOSEPHSON NON-LINEARITY

In recent times, progress in the field of quantum technologies and advancements in detection experiments have made the detection of extremely weak signals in the microwave frequency spectrum essential.

Parametric amplifiers have been very successful in recent years, extensively studied and proven to be highly successful in the microwave regime. Parametric amplifiers are appreciated for their ability to improve sensitivity in detecting weak signals, finding applications in various fields, including quantum optics, qubit readout, and single-photon detection in microwaves. They offer the important advantage of high gain, allowing them to approach or surpass the quantum noise limit.

The concept of parametric amplification has roots dating back in time, but significant early experiments occurred in the 1960s. In the optical domain, the first optical parametric amplifiers (OPAs) were developed [32–35], while in the realm of microwaves, initial steps towards parametric amplification were taken using varactor diodes as nonlinear elements, notably at Bell Laboratories. A few years later, in the mid-1970s, the first theoretical studies and experimental investigations of microwave parametric amplification using Josephson junctions emerged [36]. The first to achieve this goal were Yurke [37] and his research team at the end of the 1980s, also at Bell Laboratories. Despite the importance of this result, its value was underestimated until the beginning of the new millennium due to the lack of direct applications for cryogenic amplifiers.

The phenomenon of parametric amplification is based on the concept of wave mixing induced by the non-linearity present in the circuit. A strong EM signal, known as pump tone, is sent, which interacts with other (weak) signals. Within the device, EM waves at different frequencies can interact and combine, exchanging energy and generating new spectral components. The fundamental aspect is the extraction of energy from the pump tone, which is then directed towards the band of interest.

The mentioned non-linearity can be introduced in various ways, influencing both the device's performance and its physical properties, and sometimes even the fabrication techniques. The most commonly used types of non-linearity are Josephson non-linearity using Josephson Junction (JJ) [36], kinetic inductance [38], and many others in the field of optics. We focus exclusively on non-linearities in the microwave field, particularly on those introduced by the Josephson effect.

Other geometries are dictated by the adopted circuit topology, i.e., whether one decides to place the JJ (or a nonlinear medium in general) inside a resonator (with a certain quality factor Q) or within a series array of junctions. Both methods aim primarily to enhance stimulated emission, achieved by increasing the interaction time between pump and signal waves inside the nonlinear medium. This example is also derived from LASERs (Light Amplification by Stimulated Emission of Radiation), where pump radiation is "trapped" in the resonant cavity.

In the first case, the technique known as resonant amplification is used, yielding JPA devices [39]. Essentially, improving the Q of the resonator forces each photon to pass through the JJ on average Q times before leaving the resonator, thereby increasing nonlinear interaction. This first type is simpler to implement but has a relatively narrow bandwidth around the resonator's characteristic frequency. In these devices, the interaction between the circulating photons and a small number of nonlinear elements is enhanced by means of a resonator with a high quality factor which effectively limits the operating band. Additionally, since the Josephson non-linearity is realized with few Josephson junctions, it will consequently have a small saturation power [39]. Moreover, the non-idealities of the interaction, represented by non-linearities of a higher order than the engineered one, can cause distortions of the output squeezed quantum field.

To overcome these well-known limitations, superconducting technology has approached the second type, the so-called Josephson Traveling Wave Parametric Amplification.

J-TWPA consists of many cells in series containing nonlinear elements with a Josephson-based core and exploiting the device length to increase wave mixing and hence gain. In Fig. 2, an electrical equivalent model of the N elementary cells composing an JTWPA is shown. The central conductor of the coplanar waveguide is a chain of rf-SQUIDs composed of a geometrical inductor Lg, a Josephson junction of critical current Ic, and capacitance CJ. The line is capacitively shunted to ground by ground capacitors Cg. The distribution of non-linearity over the entire device and the elimination of resonant structures allow the generation of fields with substantial squeezing in a high dynamic range and an emission of broadband microwave entangled states [40, 41].

It has a much wider bandwidth, a few GHz, and also a larger saturation power since each JJ is excited only once. On the other hand, a complex realization is required since the device must be engineered to ensure phase (or momentum) conservation, caused by different phase velocities of the signal and pump photons, given their large difference in frequency.

Drawing from dispersion engineering techniques, well established in quantum optics and photonics, where the refractive index is modified to manipulate the momentum of a transmitted signal, O'Brien's group has devised a solution to the phase misalignment problem. They inserted resonators at regular intervals along the TWPAs, useful for slowing down the pump's phase velocity, adapting the device's phase through its wave vector. This technique is known as Resonant Phase Matching (RPM) [42]. Finally, another valid method that guarantees a wide bandwidth and a wide dynamic range, achievable again through the Josephson effect, is known as superconducting nonlinear asymmetric inductive element (SNAIL) [43]. The SNAIL is a nonlinear element composed of a superconducting ring formed by a small JJ and several larger junctions in parallel. State-of-the-art JTWPAs have shown phase-insensitive amplification with high gain values (up to 20 dB) and wide

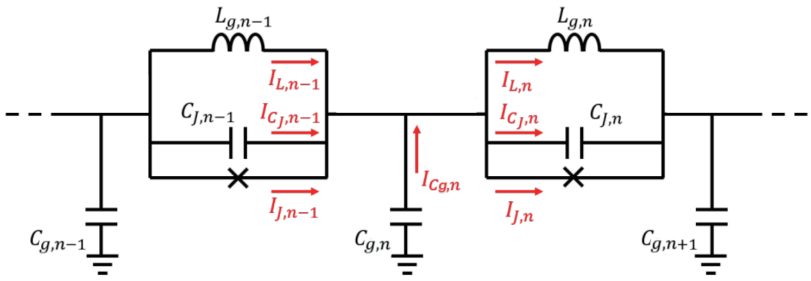

FIGURE 2. Representation of the electrical equivalent of the N elementary cells composing an JTWPA. The central conductor of the coplanar waveguide is a chain of rf-SQUIDs composed of a geometrical inductor L_g and a Josephson junction of critical current I_c and capacitance C_J. The line is capacitively shunted to ground by ground capacitors C_g.

bandwidths (3 GHz) at cryogenic temperatures, and have the potential to approach the SQL regime characterized by a number of added noise photons equal to $n_{amp} = 0.5$ for phase-insensitive operating mode [44]. It is emphasized here, as reported in [45], that a phase-sensitive linear amplifier has the possibility of exceeding the threshold of the SQL, obtaining an amplification without the added noise of a single quadrature, and paying the price of a deamplification of the conjugate quadrature. The SQL is a fundamental noise limit that arises from the principles of quantum mechanics. It represents the minimum possible noise that an amplifier can achieve while still obeying the Heisenberg uncertainty principle [46]. These features pave the way for the generation of TMSV states, in which two EM modes are entangled, with a large correlation between quadratures which cannot be achieved classically. This makes TMSV states an ideal resource for applications in quantum radar. Proper biasing condition can change the overall transmissivity of an RF-SQUID-based JTWPA since the series inductance of the Transmission Line (TL) depends on the value of the Josephson inductance. As an example, a change of the DC current flowing into the TL, I_{DC}, can cause a modulation of its characteristic impedance $Z = \sqrt{L(I)/C}$ where C is the capacitance to ground per unit length, and $L(I)$ is the series inductance per unit length, which is current dependent. For this reason, a measure of the reflected and transmitted power in terms of scattering parameters as a function of I_{DC} can give important hints about the impedance matching of the transmission line and how this feature gets modified by the biasing.

3.1. TWPAs Gain

To better understand how the process of parametric amplification occurs in the TWPA, we will see how it unfolds following a comprehensive approach similar to that described in [47]. For the TWPA in question, a distributed parameter model is utilized along a coplanar waveguide with a certain periodicity, with the Josephson inductance serving as the nonlinear element. The starting point is the nonlinear relationship of the Josephson inductance dependent on current, which can be generally written as:

$$L(i) = L_J(1 + \eta i) \tag{4}$$

where η is a proportionality constant that accounts for the current variation along the JJ (Josephson Junction), and through some mathematical steps, it can be shown that $\eta = \frac{I^2}{2I_C^2}$ [36].

Furthermore, for this analysis, only the frequencies ω_p, ω_s, and ω_i are considered, representing the pump, signal, and idler frequencies, respectively, and are linked by the relationship:

$$\omega_s + \omega_i = \omega_p \tag{5}$$

Moving on to the equations characterizing the transmission lines, namely the telegrapher's equations, and performing mathematical manipulations on them, we obtain the d'Alembert wave equation:

$$\frac{\partial^2 i}{\partial z^2} = \frac{1}{v_{ph}^2}\frac{\partial^2 i}{\partial t^2}(i + \eta i^2) \tag{6}$$

where v_{ph} is the phase velocity of the wave propagating along the transmission line.

By considering simplified situations for the current i and through some mathematical steps, it is possible to obtain mixed products from which a parameter can be derived that accounts for the growth constant of the amplified waves, namely:

$$\alpha_0 = \frac{\eta I_{30}}{2}\sqrt{k_1 k_2} \tag{7}$$

From this, we can derive that:

$$G = 20 \log \cosh(\alpha_0 l) \text{ [dB]} \tag{8}$$

where G is the gain in dB, and l is the length of the line. Essentially, an approximate model for the gain G in a TWPA under small perturbation conditions has been obtained. This gain is derived from a small signal analysis and is an approximate solution, but it well explains that for small lengths, a gain is achieved according to the law mentioned above.

3.2. TWPA S-Parameters

In this subsection, we will briefly explain how to obtain the generalized multi-port scattering matrix for an arbitrary network of parametrically coupled modes (also valid for resonantly coupled modes). This is achieved through a matrix of equations of motion (EoM) of the coupled modes M, as described in [48, 49]. In the general case, a good starting point can be the equations of the TWPA relating the complex amplitudes of the signal's propagating normal modes, a_{s+}, to its

parametrically coupled idler, $a_{i+}{}^{*}$:

$$\frac{da_{s+}}{dz} = j\kappa k_s \frac{a_p^n}{n} a_{i+}^* \tag{9}$$

$$\frac{da_{i+}{}^{*}}{dz} = j\kappa k_i \frac{a_p^n}{n} a_{s+}^* \tag{10}$$

where a_p is the pump amplitude, assuming that it is constant along the transmission line (the so-called "stiff pump approximation"), where "*" denotes the complex conjugate, and the signal and idler frequencies and propagation constants are parametrically constrained by the pump values, from the relationships:

$$n\omega_p = \omega_s + \omega_i \tag{11}$$

$$nk_p = k_s + k_i \tag{12}$$

with $n = 1$ in the case of using 3-wave and $n = 2$ for 4-wave mixing.

Equations (9) and (10) represent a system of first-order differential equations, which interconnects the energies of the two coupled modes, signal and idler, propagating along a transmission line.

Equations (11) and (12) impose the energy conservation and momentum conservation (known as "phase-matching"), respectively. The coupling constant k is generated by modulating the inductance in series at frequency ω_p. In the specific case of TWPAs, this process is carried out using transmission lines composed of arrays of Josephson junctions [36], which provide nonlinear inductances that can be modulated through pump currents.

An interesting observation that can be derived from the EoM is the complex spatial dependence that advances the phase of a moving wave in space, intensifying through the parametric coupling between signal and idler wave pairs. This phenomenon is particularly evident in TWPAs, where coupling is driven by frequency mixing induced by the pump wave, with a phase $\phi_p(t,z) = k_p z - \omega_p t$, which depends on both time t and distance z along the line. Furthermore, from the relation (12) linking the propagation constants, it is possible to deduce the relative phase between the signal and idler waves.

By transforming the EoM, using Fourier transform, it is possible to obtain, more simply, the solutions of the coupled multimodal system parametrically. Furthermore, by performing further manipulations, it is possible to derive the following scattering parameter matrix:

$$S = jKM^{-1}K - \mathbb{I} \tag{13}$$

where matrix M synthesizes the motion equations in the frequency domain, illustrating how energy transfer occurs between oscillating fields and their frequency combinations. Matrix K describes how energy is dissipated or absorbed by the circuit components through the circuit in/out ports.

A noteworthy consideration between the above definition and classic S parameters is that here the scattering parameters are defined as the ratio of the output and input amplitudes of the selected modes normalized to energy quanta, $\hbar\omega_k{}^s$, namely:

$$S_{jk} = \frac{a_j^{out}}{a_k^{in}} \tag{14}$$

whereas, classic scattering parameters are commonly defined by the ratio of equivalent voltage amplitudes, i.e.:

$$vanTreesS_{jk} = \frac{V_j^{out}}{V_k^{in}} \tag{15}$$

Therefore, by considering different definitions between the two formulae, a process with unit gain according to the convention above will be associated with a gain factor in the common definition of scattering parameters in electronic engineering. For further details, see [48].

3.3. Squeezing

To quantify the squeezing of the devices of interest, we included a mathematical treatment and considerations on the quantum model of JTWPA. As mentioned earlier, the quantum states produced by typical JTWPAs induce a two-mode squeezed vacuum state $|\Psi\rangle$ through non-degenerate spontaneous parametric down-conversion of a pump photon, if now we rewrite Eq. 1 as:

$$|\Psi\rangle_{SI} = \sum_{n=0}^{\infty} \sqrt{\cosh(r)}\, e^{in\theta(r)} |n\rangle_S |n\rangle_I \tag{16}$$

in which $|\Psi\rangle_{SI}$ denotes the two-mode squeezed vacuum state in the Fock-state basis of the signal (S) and idler (I) output fields. The parameter r, representing the modulus of the squeezing parameter, depends on the metamaterial components and frequency characteristics, elucidated by a circuit-Quantum ElectroDynamics (c-QED) model [50]. The squeezing of the two quadratures q_j and p_j:

$$q_j = a_j + a_j^\dagger, \quad p_j = i(a_j^\dagger - a_j) \tag{17}$$

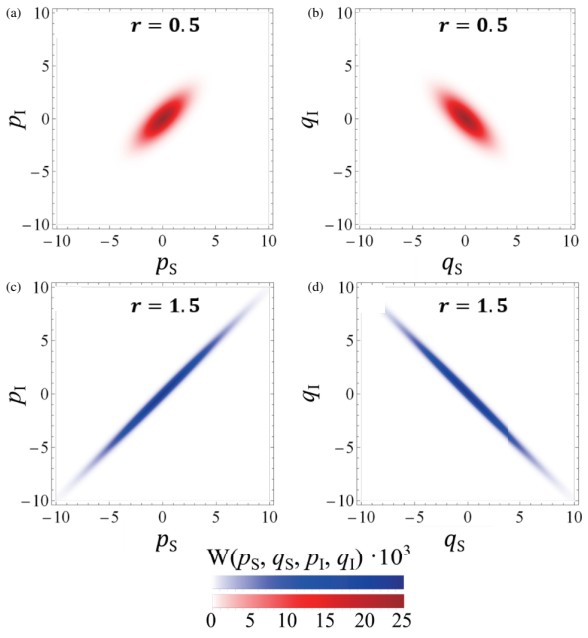

FIGURE 3. Wigner distributions of the TMSV states for different values of the squeezing parameter. In (a) and (b), $r = 0.5$, while in (c) and (d), $r = 1.5$.

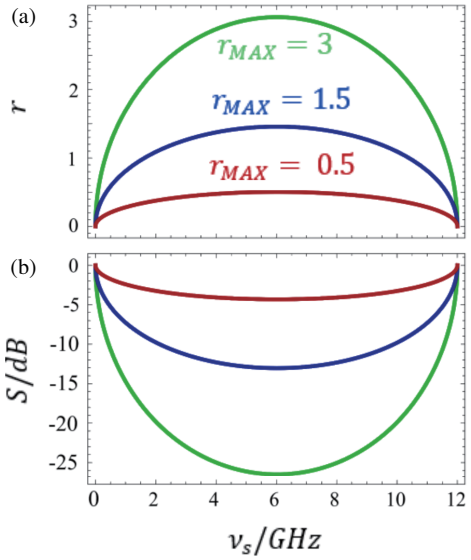

FIGURE 4. (a) The modulus of the squeezing parameter r and (b) the squeezing spectrum S as a function of the signal frequency ν_s. The peak S values of r for the three curves are 0.5 (red), 1.5 (blue), and 3 (green), resulting in maximum squeezing levels of -4.5 dB, -13.2 dB, and -26.5 dB, respectively. All curves are computed using the model from [50] with a pump frequency of 12 GHz.

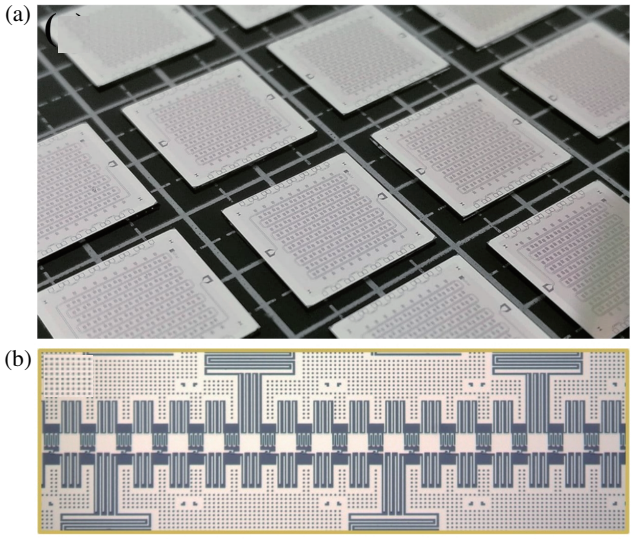

FIGURE 5. (a) Picture of the fabricated JTWPA chip with a size 10×10 mm^2. (b) Detail of the fabricated JTWPA.

of the TMSV state generated by a JTWPA with r values of 0.5 and 1.5 is depicted in Figs. 3 (a), (b) and (c), (d), respectively, using their associated Wigner distributions. Here, a_j and $a_j^\dagger$ are the bosonic creation and annihilation operators for the j-th mode. Experimental evidence has shown that the squeezing parameter r in JTWPAs can reach values up to approximately 3, corresponding to a gain G about 20 dB [50–52]. This parameter determines the squeezing capabilities across the bandwidth as illustrated in Fig. 4(a), where different experimental conditions lead to varying r_{MAX} values. Fig. 4(b) shows the corresponding squeezing spectrum S. Higher values of r indicate more intense squeezing. The apical S values of r for the three curves are 0.5 (red), 1.5 (blue), and 3 (green), leading to a maximum squeezing magnitude of -4.5 dB, -13.2 dB, and -26.5 dB, respectively. All the curves have been calculated following the model in [50] and supposing a pump frequency of 12 GHz. The squeezing between two quadratures under low gain conditions ($r = 0.5 - 1.5$, corresponding to $G = 7.2$ dB -1.1 dB) is visually represented in Figs. 4(a) and 4(b).

4. EXPERIMENTAL PRELIMINARY SCATTERING PARAMETERS FOR THE DEVELOPED JTWPA

We report the performance and the first characterization of our recently developed JTWPA operating as a TMSW entangled quantum source, shown in Fig. 5. The signals of interest, called TMSV states, exploit a particular type of continuous-variable entanglement, causing sequences of TMSV pulses to follow a Gaussian distribution, which can be measured through the I-Q quadrature voltages. The representation of a state within this mapping is not static due to the influence of electronic noise; consequently, the states are observed not to be localized at a fixed point but rather distributed within a certain area. This distribution is uniquely defined by its mean and covariance matrix, which respectively describe its center and dispersion in the variable space. Essentially, as the input variable to the devices, we send the 'vacuum state' (state with minimum uncertainty). This refers to a specific condition of an EM field where the photon number is zero, yet there exists zero-point energy ($1/2h\nu$). This zero-point energy is a manifestation of the intrinsic quantum fluctuations of the field. The existence of zero-point energy is closely related to the uncertainty principle: indeed, the idea that the energy in a quantum mode can never be exactly zero due to the uncertainty relation [46]. For the generation of such signals, parametric devices as JTWPA are used, which perform a process called spontaneous down-conversion (SPDC). It is an instantaneous nonlinear optical process that converts a higher-energy photon (pump photon) into a pair of lower-energy photons (signal photon and idler photon), in accordance with the laws of energy conservation and conservation of momentum. It is an important process in quantum physics for generating entangled photon pairs. A first characterization of the RF-SQUIDs based JTWPA, biased by a DC current in order to promote three-wave mixing (3WM) interactions by tuning the Josephson non-linearity, is performed by measuring the output idler tone power, generated via 3WM and 4WM. The experiment is carried on into a dry dilution refrigerator (see the experimental setup in Fig. 6), manufactured by Leyden Cryogenics capable of reaching a base temperature of 10 mK. The JTWPA inside its packaging (see Fig. 7) is positioned at the bottom of the cryostat, in the coldest stage (in the so called "Mixing chamber"), in order to maintain the thermal noise contribution as low as possible and avoid the destruction of the generated entanglement.

The device is fed with a driving pump frequency $\omega_p/2\pi = 6.75$ GHz and a signal frequency $\omega_s/2\pi = 3.3$ GHz with signal power $P_s = -64$ dBm.

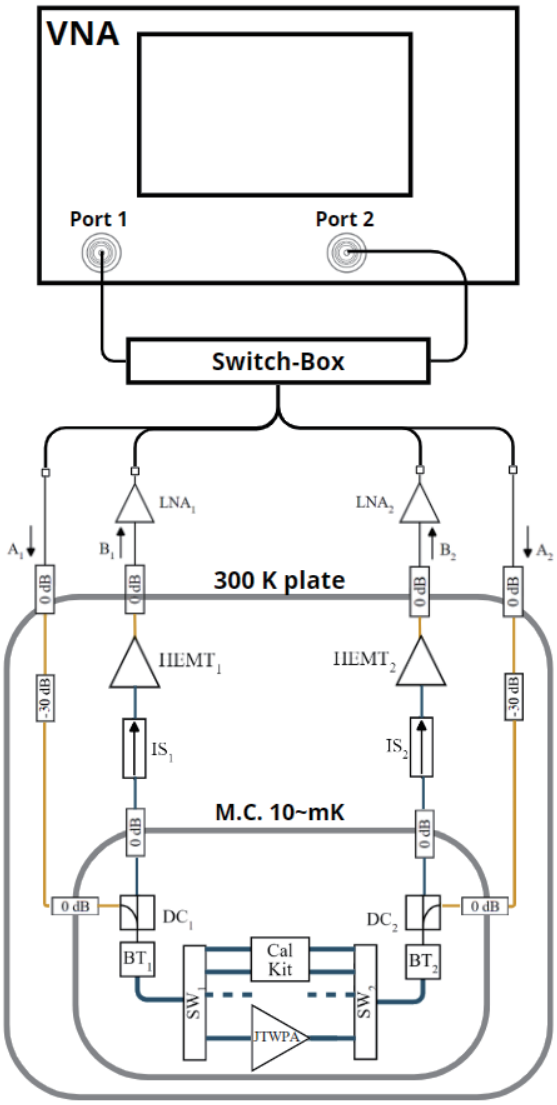

FIGURE 6. Experimental cryogenic setup, composed of a dry dilution refrigerator with a base temperature of 10 mk, used to acquire data with a VNA.

Thanks to the low losses of the JTWPA based on three-wave mixing (3WM) design, estimated at around 0.6 dB, the generation of frequency entangled microwave signals, starting from the vacuum state, spaced in frequency up to $(\omega_i - \omega_s)/2\pi = 17$ MHz and with a (base 2) logarithmic negativity $E = 0.86 \pm 0.21$, has been demonstrated [53]. For the single frequency operation mode instead ($\omega_i = \omega_s$), 2.4 ± 0.7 dB of quantum squeezing has been achieved. Furthermore, in Fig. 8, the comparison between the idler measured powers for the 3WM and 4WM mixing processes vs the DC bias current ranging between -50 µA and $+50$ µA is reported. The 3WM and 4WM processes are shown in Figs. 9(a) and 9(b), respectively. The pump tone is set to 6.75 GHz with the power of -52 dBm while the signal tone is set to 3.3 GHz with the power of -64 dBm, which sets the 3WM idler frequency to 3.45 GHz and the 4WM idler to 10.2 GHz. The possibility to send a DC current to the RF-SQUIDS in the TWJPA allows to tune their nonlinearity in order to generate 4WM and 3WM processes. When the DC bias current flows through the nonlinear transmission line, the inductance of each cell changes, in a periodic manner due to the SQUID behavior. The periodicity corresponds ideally, in our device, to 46 µA, which is the distance between the second and fourth minima, Fig. 8.

According to the 3WM process, the frequency of the idler is equal to $\omega_i/2\pi = 3.45$ GHz so that $\omega_s + \omega_i = \omega_p$ is verified.

The proposed microwave QI detection schemes implement homodyne detection similar to what is commonly used in optical counterparts [54]. Experimental detection protocols, implemented in cryogenic microwave apparatuses, typically use a concatenation of quantum amplifiers followed by cryogenic high electron mobility transistor (HEMT) amplifiers. From the Friis formula, for this type of condition [55], the nominal value of the total noise depends mainly on the noise properties of the first amplifier, which can again take advantage of the peculiar features of the Josephson amplifiers.

Figure 10 shows two contour plots of very preliminary data of our developed JTWPA, related to the scattering matrix elements S_{21} and S_{11} parameters in a frequency range between 4 GHz and 12 GHz and in an I_{DC} range between -20 μA and 20 μA. The spectra show several dips related to the resonating condition which get more or less deep depending on the value of I_{DC}. These features testify a loss of transmitted energy localised in different narrow frequency bands that can be explained taking into account a multiple resonant mechanism caused by the geometrical features of the device. Supposing an imperfect impedance matching between two subsequent sections of the transmission line, we can think of the interfaces as the input and output ports of a resonator of length a, equal to the length of the section taken into account. In Fig. 11, the detail of the S_{11} parameter in a narrow region is around 7.5% GHz for I_{DC} values from -20 uA to 20 uA. A clear harmonic dependence of the resonating condition as a function of I_{DC} is visible.

Experimental results for the fabricated JTWPA in terms of gain vs frequency over the 0 to 12 GHz frequency band, as a function of the pump current I_p normalized on the critical current I_c of Josephson junctions composing the referenced device, are reported in Fig. 12. For a signal central frequency equal to 6 GHz, a maximum gain of 32.40 dB and maximum bandwidth of 4 GHz at the 3 dB threshold level, identified with the dashed lines, are obtained [66].

5. JTWPA-BASED MICROWAVE QUANTUM RADAR PERFORMANCE

Microwave quantum radar leverages the principles of quantum mechanics to enhance detection performance compared to classical radar systems. It utilizes phenomena such as quantum entanglement and squeezed states to reduce noise and improve system sensitivity. Here is an overview of the operating principle and the range of a microwave quantum radar.

5.1. Operating Principle

The quantum radar, unlike a classical radar that uses a conventional EM signal, employs pairs of entangled photons, known as

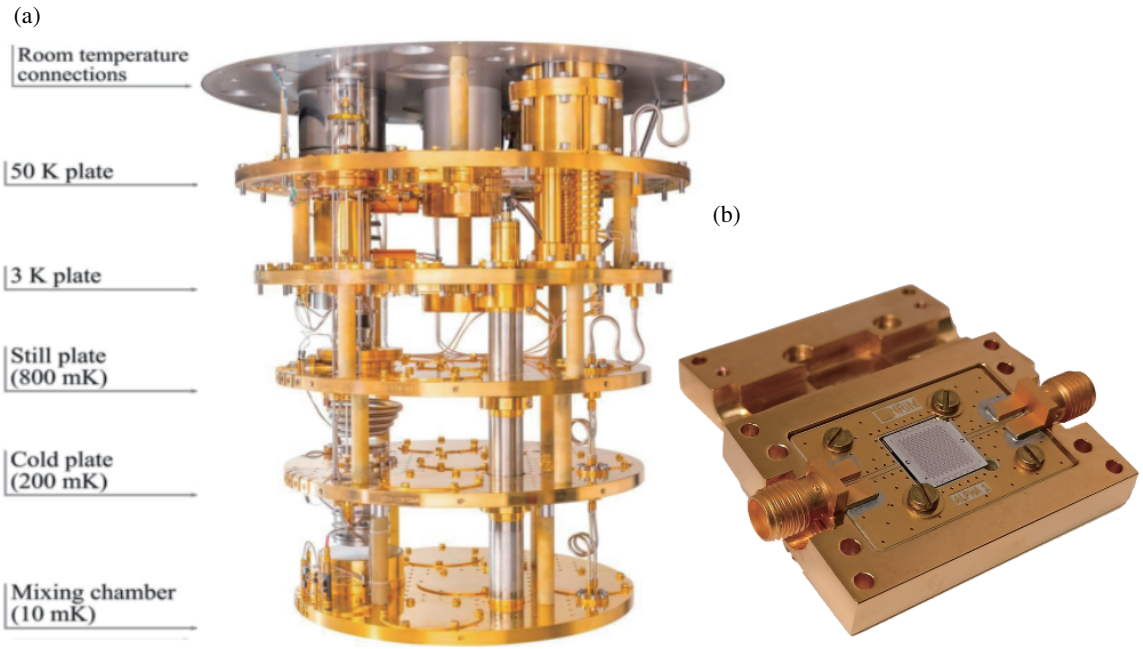

FIGURE 7. (a) Cryostat dry refrigerator CF-CS110-500 used for the experiment, (b) JTWPA source for TMSV states, fabricated at INRIM, with its packaging designed for cold applications.

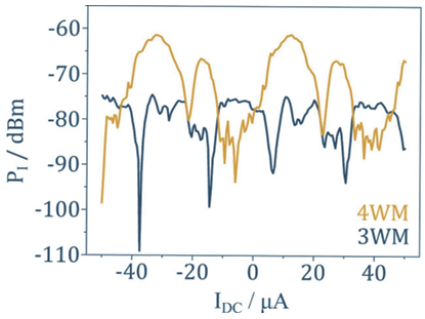

FIGURE 8. Measured power of the 3WM (blue) and 4WM (yellow) idlers vs the DC bias current ranging between −50 μA and +50 μA.

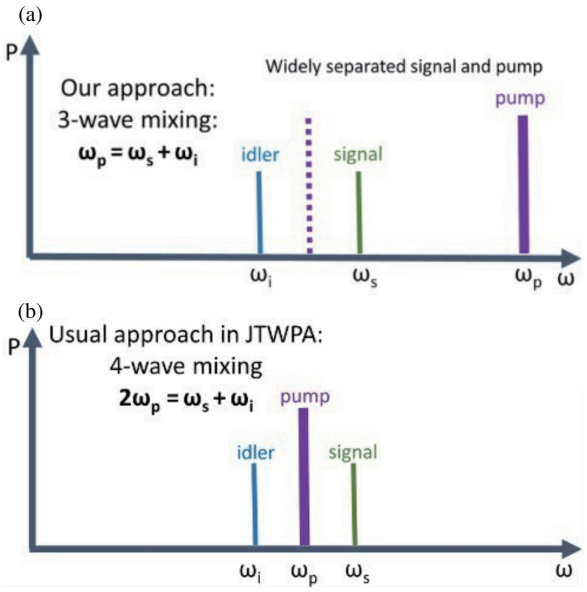

FIGURE 9. (a) 3WM and (b) 4WM idler tones measured by a spectrum analyzer. The pump tone is set to 6.75 GHz with a power of −52 dBm and the signal tone is set to 3.3 GHz with a power of −64 dBm; this sets the 3WM idler frequency to 3.45 GHz and the four-wave mixing (4WM) idler one to 10.2 GHz.

the idler photon and signal photon. The quantum states of these photons are correlated such that the state of the entire system is described by their linear combination. The signal photon is sent towards a region where a target might be present, while the idler photon is measured immediately or retained within the system to be later compared with the returning signal photon. In this way, the reference and received signals are used to simultaneously measure their correlation. In Fig. 13, the schematic block diagram of a microwave quantum radar prototype is shown.

This protocol utilizes TMSV state signals. Despite the loss of entanglement due to the interaction with the environment (including amplification), the QTMS radar aims to exploit the correlation caused by entanglement to detect signal photons in noise by calculating the correlation multiple times [2, 22]. As mentioned in Section 3, the source generating the TMSV signals is the JTWPA, powered solely by the pump. In the output, two signals (shown in blue and yellow) are obtained and travel through the amplification line. The signal photon is then propagated while the idler photon is digitized and measured (using the so-called joint measurement). Obviously, once the signal has been sent, if reception occurs, the process of comparing the returning signal with the measured idler can be carried out. To enhance performance in the receiving stage, various techniques have been introduced over the years to achieve optimal receivers [56–60].

.

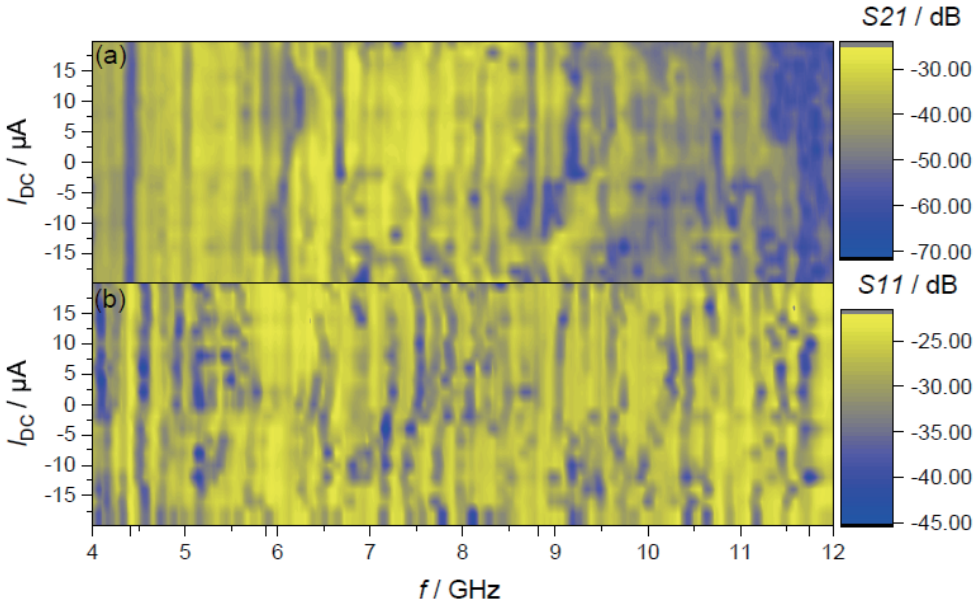

FIGURE 10. Very preliminary characterization of JTWPA in terms of S_{21} and S_{11} scattering matrix elements over the range $4 - 12$ GHz for I_{DC} values from -20 μA to $+20$ μA.

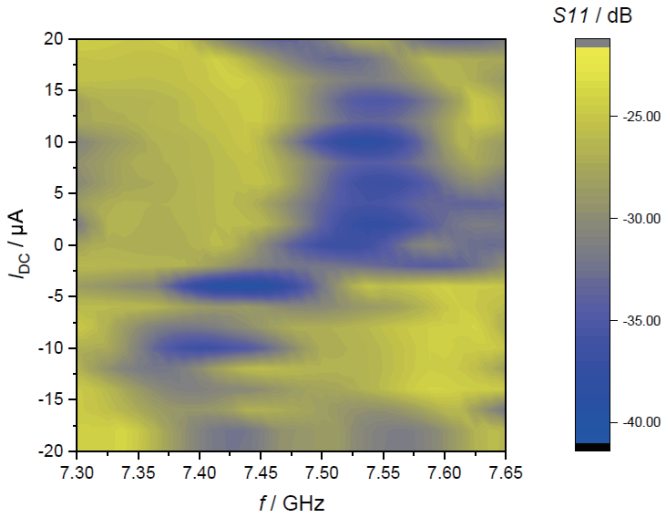

FIGURE 11. Detail of the S_{11} parameter in the region around 7.5 GHz for I_{DC} values from -20 μA to $+20$ μA.

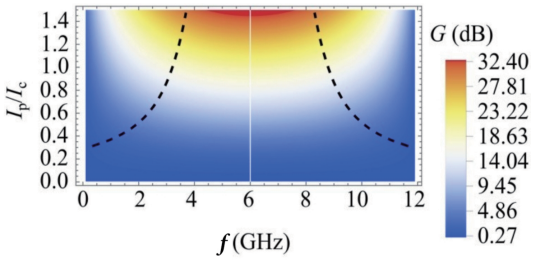

FIGURE 12. Gain spectrum vs frequency, expressed in dB, as a function of the pump current I_p normalized on the critical current I_c of the Josephson junctions composing the referenced device. The dashed lines identify the bandwidth of this device at the 3 dB threshold level.

5.2. Maximum Range of Microwave Quantum Radar

The maximum range of a microwave quantum radar depends on various factors similar to those of classical radars, with additional enhancements from quantum technologies. The transmitted power directly affects the range. Higher power increases the range. As in classical radars, the gain of the transmitting and receiving antennas affects the range. High-gain antennas can transmit and receive higher signals. The wavelength of the microwave radiation determines the radar's ability to penetrate obstacles and atmospheric conditions. Lower frequencies (longer wavelengths) tend to have a greater range in adverse atmospheric conditions. The radar cross-section of the target influences the amount of reflected signal. Larger or more reflective targets can be detected at greater distances. Using entanglement and squeezed states allows for noise reduction and SNR improvement, increasing the effective range of the radar. Quantum techniques can enable effective detection at greater distances than classical radars with the same power and gain setup. Since the MQR based on TMSV can be considered a modified version of the classical noise radar, the equation of the maximum radar range for a quantum radar based on a JTWPA can be derived by Eqs. (1), (4)–(8) of Chapter 2 in [61], from Eq. (17) of [62], Eq. (20) of Chapter 2 in [63], and [64].

Starting from these equations, it occurs:

$$R_{max} = \left(\frac{G A_e \sigma P_s}{(4\pi)^2 P_n (SNR)^Q_{min}} \right)^{1/4} \tag{18}$$

where R_{max} is the maximum radar range; G is the antenna gain; A_e is the effective antenna area; σ is the target radar cross-section; P_s and P_n are the signal power and noise power, respectively; and $(SNR)^Q_{min}$ is the minimum signal to noise ratio at the input of the receiver.

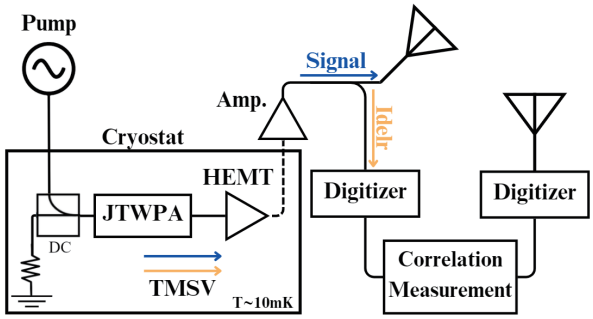

FIGURE 13. Block diagram of the microwave quantum radar prototype.This is a simplified block diagram, illustrating only the most important elements of the IN/OUT lines of the cryostat. The process begins with the generation of the pump signal, which is directed towards the JTWPA (Josephson Traveling Wave Parametric Amplifier). The output from the JTWPA produces TMSV signals. These signals are partly directed to the transmitter (signal photons) and partly digitized and directly measured (idler photons) through the so-called joint measurement. Finally, on the receiver side, potential returning signal photons are expected and compared through the correlation of the stored signal and idler photons.

TABLE 1. MQR performance based on the developed JTWPA and comparison with MQR parameters based on JPA and JPC.

Parameters	JPA [10]	JPC [65]	JTWPA [This work]
Antenna bandwidth (GHz)	X-band	C-band	S-band
Antenna Gain (dB)	15	15	15
Target RCS (m^2)	1.0	1.0	1.0
Bandwidth (MHz)	1.0	20	3,000
JPA/JTWPA Power Gain (dB)	20	30	30
Signal Gain (dB)	96	94	83.98
Signal Power (dBm)	−82	−128	−64
Pump frequency (GHz)	13.6821	16.89	6.75
Signal frequency (GHz)	7.5376	10.09	3.3
Idler frequency (GHz)	6.1445	6.8	3.45
Signal to Noise Ratio (dB)	−19	−18	−13.48
Range (m)	0.5	1	82.2

In Table 1, the performance of a Microwave Quantum Radar exploiting the JTWPA developed and characterized at INRiM, Italy, jointly with the comparison to MQR parameters based on JPA and JPC, is reported. The parameter RCS, that is the receiver cross section denoted σ, is a measure of how detectable an object is by a radar. In particular, for the developed JTWPA operating as a non-classical entangled-photons source over the S-band, a detection range equal to 82.2 meters is obtained, which represents a greater value than the values reported in [10] and [65]. Our maximum radar range value above the limit of 2 m imposed by the JPA technology paves the way to a real-world microwave quantum radar.

6. CONCLUSION

In this study, we have conducted an investigation into a potential technology for the implementation of a microwave quantum radar. We started the theoretical study of the quantum illumination protocol and then moved on the analysis of a device that generates the entangled signals of interest, JTWPA. The JTWPA, in fact, exhibits wider operational bandwidth and higher efficiency than traditional JPA. Our calculations indicate that JTWPAs can operate effectively across a wide range of frequencies, which is advantageous for MQR applications requiring different operational conditions. The wide bandwidth allows for more flexible and powerful MQR systems, addressing the range and power output limitations of JPAs.

In addition to a theoretical physical study, we conducted a modeling and a very preliminary characterization of the JTWPA, based on simulations and application of mathematical models. This allowed us to obtain information on the possible range achievable using JTWPAs.

Despite the promising results, there is still room for further research to optimize JTWPAs for complex quantum radar systems. Future work could focus on increasing the entanglement and exploring hybrid systems that combine the strengths of JTWPAs with other quantum technologies. Additionally, refining the design to further reduce noise and improve operational efficiency will be critical for advancing the technology.

In conclusion, the development and application of JTWPAs represent a significant milestone in the evolution of quantum radar technology. Our comprehensive approach, involving simulations, theoretical calculations, and experimental validations, including detailed analysis of scattering parameters, has demonstrated that JTWPAs are not only viable quantum sources but also have the potential to revolutionize the field of quantum sensing. The findings from this study pave the way for future advancements and practical implementations of JTWPAs in various high-impact applications.

REFERENCES

[1] Dowling, J. P., "Quantum optical metrology — The lowdown on high-N00N states," *Contemporary Physics*, Vol. 49, No. 2, 125–143, 2008.

[2] Lloyd, S., "Enhanced sensitivity of photodetection via quantum illumination," *Science*, Vol. 321, No. 5895, 1463–1465, 2008.

[3] Hao, S., H. Shi, W. Li, J. H. Shapiro, Q. Zhuang, and Z. Zhang, "Entanglement-assisted communication surpassing the ultimate classical capacity," *Physical Review Letters*, Vol. 126, No. 25, 250501, 2021.

[4] Shapiro, J. H., "The quantum illumination story," *IEEE Aerospace and Electronic Systems Magazine*, Vol. 35, No. 4, 8–20, 2020.

[5] Karsa, A., G. Spedalieri, Q. Zhuang, and S. Pirandola, "Quantum illumination with a generic gaussian source," *Physical Review Research*, Vol. 2, No. 2, 023414, 2020.

[6] Sorelli, G., N. Treps, F. Grosshans, and F. Boust, "Detecting a target with quantum entanglement," *IEEE Aerospace and Electronic Systems Magazine*, Vol. 37, No. 5, 68–90, 2021.

[7] Shapiro, J. H., "Extended version of van trees's receiver operating characteristic approximation," *IEEE Transactions on Aerospace and Electronic Systems*, Vol. 35, No. 2, 709–716, 1999.

[8] Lopaeva, E. D., I. R. Berchera, I. P. Degiovanni, S. Olivares, G. Brida, and M. Genovese, "Experimental realization of quantum illumination," *Physical Review Letters*, Vol. 110, No. 15, 153603, 2013.

[9] Pirandola, S., B. R. Bardhan, T. Gehring, C. Weedbrook, and S. Lloyd, "Advances in photonic quantum sensing," *Nature Photonics*, Vol. 12, No. 12, 724–733, 2018.

[10] Luong, D., C. W. S. Chang, A. M. Vadiraj, A. Damini, C. M. Wilson, and B. Balaji, "Receiver operating characteristics for a prototype quantum two-mode squeezing radar," *IEEE Transactions on Aerospace and Electronic Systems*, Vol. 56, No. 3, 2041–2060, 2019.

[11] Alibart, O., V. D'Auria, M. D. Micheli, F. Doutre, F. Kaiser, *et al.*, "Quantum photonics at telecom wavelengths based on lithium niobate waveguides," *J. Opt.*, Vol. 18, 104001, 2016.

[12] Lee, K. F., J. Chen, C. Liang, X. Li, P. L. Voss, and P. Kumar, "Generation of high-purity telecom-band entangled photon pairs in dispersion-shifted fiber," *Optics Letters*, Vol. 31, No. 12, 1905–1907, 2006.

[13] Eichler, C., D. Bozyigit, C. Lang, M. Baur, L. Steffen, J. M. Fink, S. Filipp, and A. Wallraff, "Observation of two-mode squeezing in the microwave frequency domain," *Physical Review Letters*, Vol. 107, No. 11, 113601, 2011.

[14] Flurin, E., N. Roch, F. Mallet, M. H. Devoret, and B. Huard, "Generating entangled microwave radiation over two transmission lines," *Physical Review Letters*, Vol. 109, No. 18, 183901, 2012.

[15] Flurin, E., N. Roch, J.-D. Pillet, F. Mallet, and B. Huard, "Superconducting quantum node for entanglement and storage of microwave radiation," *Physical Review Letters*, Vol. 114, No. 9, 090503, 2015.

[16] Menzel, E. P., R. D. Candia, F. Deppe, P. Eder, L. Zhong, M. Ihmig, M. Haeberlein, A. Baust, E. Hoffmann, D. Ballester, *et al.*, "Path entanglement of continuous-variable quantum microwaves," *Physical Review Letters*, Vol. 109, No. 25, 250502, 2012.

[17] Ku, H. S., W. F. Kindel, F. Mallet, S. Glancy, K. D. Irwin, G. C. Hilton, L. R. Vale, and K. W. Lehnert, "Generating and verifying entangled itinerant microwave fields with efficient and independent measurements," *Physical Review A*, Vol. 91, No. 4, 042305, 2015.

[18] Fedorov, K. G., L. Zhong, S. Pogorzalek, P. Eder, M. Fischer, J. Goetz, E. Xie, F. Wulschner, K. Inomata, T. Yamamoto, *et al.*, "Displacement of propagating squeezed microwave states," *Physical Review Letters*, Vol. 117, No. 2, 020502, 2016.

[19] Fedorov, K. G., S. Pogorzalek, U. L. Heras, M. Sanz, P. Yard, P. Eder, M. Fischer, J. Goetz, E. Xie, K. Inomata, *et al.*, "Finite-time quantum entanglement in propagating squeezed microwaves," *Scientific Reports*, Vol. 8, No. 1, 6416, 2018.

[20] Westig, M., B. Kubala, O. Parlavecchio, Y. Mukharsky, C. Altimiras, P. Joyez, D. Vion, P. Roche, D. Esteve, M. Hofheinz, *et al.*, "Emission of nonclassical radiation by inelastic cooper pair tunneling," *Physical Review Letters*, Vol. 119, No. 13, 137001, 2017.

[21] Grimsmo, A. L. and A. Blais, "Squeezing and quantum state engineering with josephson travelling wave amplifiers," *Npj Quantum Information*, Vol. 3, No. 1, 20, 2017.

[22] Tan, S.-H., B. I. Erkmen, V. Giovannetti, S. Guha, S. Lloyd, L. Maccone, S. Pirandola, and J. H. Shapiro, "Quantum illumination with gaussian states," *Physical Review Letters*, Vol. 101, No. 25, 253601, 2008.

[23] Assouly, R., R. Dassonneville, T. Peronnin, A. Bienfait, and B. Huard, "Demonstration of quantum advantage in microwave quantum radar," *arXiv:2211.05684v1*, 2022.

[24] Macklin, C., K. O'Brien, D. Hover, M. E. Schwartz, V. Bolkhovsky, X. Zhang, W. D. Oliver, and I. Siddiqi, "A near–quantum-limited josephson traveling-wave parametric amplifier," *Science*, Vol. 350, No. 6258, 307–310, 2015.

[25] Planat, L., A. Ranadive, R. Dassonneville, J. P. Martinez, S. Leger, C. Naud, O. Buisson, W. Hasch-Guichard, D. M. Basko, and N. Roch, "Photonic-crystal josephson traveling-wave parametric amplifier," *Physical Review X*, Vol. 10, No. 2, 021021, 2020.

[26] Livreri, P., E. Enrico, L. Fasolo, A. Greco, A. Rettaroli, D. Vitali, A. Farina, C. F. Marchetti, and A. S. D. Giacomin, "Microwave quantum radar using a josephson traveling wave parametric amplifier," in *2022 IEEE Radar Conference (RadarConf22)*, 1–5, New York City, NY, USA, 2022.

[27] Livreri, P., E. Enrico, D. Vitali, and A. Farina, "Microwave quantum radar using a josephson traveling wave parametric amplifier and a phase-conjugate receiver for a long-distance detection," in *2023 IEEE Radar Conference (RadarConf23)*, 1–5, San Antonio, TX, USA, 2023.

[28] Luong, D., S. Rajan, and B. Balaji, "Quantum two-mode squeezing radar and noise radar: correlation coefficients for target detection," *IEEE Sensors Journal*, Vol. 20, No. 10, 5221–5228, 2020.

[29] Qiu, J. Y., A. Grimsmo, K. Peng, B. Kannan, B. Lienhard, Y. Sung, P. Krantz, V. Bolkhovsky, G. Calusine, D. Kim, *et al.*, "Broadband squeezed microwaves and amplification with a josephson travelling-wave parametric amplifier," *Nature Physics*, Vol. 19, No. 5, 706–713, 2023.

[30] Van Trees, H. L., *Detection, Estimation, and Modulation Theory, Part I: Detection, Estimation, and Linear Modulation Theory*, New York, NY, USA, John Wiley & Sons, 2004.

[31] Helstrom, C. W., "Quantum detection and estimation theory," *Journal of Statistical Physics*, Vol. 1, 231–252, 1969.

[32] Mollow, B. R. and R. J. Glauber, "Quantum theory of parametric amplification. I," *Physical Review*, Vol. 160, No. 5, 1076, 1967.

[33] Kroll, N. M., "Parametric amplification in spatially extended media and application to the design of tuneable oscillators at optical frequencies," *Physical Review*, Vol. 127, No. 4, 1207, 1962.

[34] Kingston, R. H., "Parametric amplification and oscillation at optical frequencies," *Proceedings of The Institute of Radio Engineers*, Vol. 50, No. 4, 472, 1962.

[35] Akhmanov, S. A. and R. V. Khokhlov, "Concerning one possibility of amplification of light waves," *Sov. Phys. Jetp*, Vol. 16, 252–257, 1963.

[36] Josephson, B. D., "Possible new effects in superconductive tunnelling," *Physics Letters*, Vol. 1, No. 7, 251–253, 1962.

[37] Yurke, B., L. R. Corruccini, P. G. Kaminsky, L. W. Rupp, A. D. Smith, A. H. Silver, R. W. Simon, and E. A. Whittaker, "Ob-

servation of parametric amplification and deamplification in a josephson parametric amplifier," *Physical Review A*, Vol. 39, No. 5, 2519, 1989.

[38] Malnou, M., J. Aumentado, M. R. Vissers, J. D. Wheeler, J. Hubmayr, J. N. Ullom, and J. Gao, "Performance of a kinetic inductance traveling-wave parametric amplifier at 4 kelvin: Toward an alternative to semiconductor amplifiers," *Physical Review Applied*, Vol. 17, No. 4, 044009, 2022.

[39] Aumentado, J., "Superconducting parametric amplifiers: the state of the art in josephson parametric amplifiers," *IEEE Microwave Magazine*, Vol. 21, No. 8, 45–59, 2020.

[40] Perelshtein, M. R., K. V. Petrovnin, V. Vesterinen, S. H. Raja, I. Lilja, M. Will, A. Savin, S. Simbierowicz, R. N. Jabdaraghi, J. S. Lehtinen, *et al.*, "Broadband continuous-variable entanglement generation using a kerr-free josephson metamaterial," *Physical Review Applied*, Vol. 18, No. 2, 024063, 2022.

[41] Esposito, M., A. Ranadive, L. Planat, and N. Roch, "Perspective on traveling wave microwave parametric amplifiers," *Applied Physics Letters*, Vol. 119, No. 12, 2021.

[42] O'Brien, K., C. Macklin, I. Siddiqi, and X. Zhang, "Resonant phase matching of josephson junction traveling wave parametric amplifiers," *Physical Review Letters*, Vol. 113, No. 15, 157001, 2014.

[43] Frattini, N. E., V. V. Sivak, A. Lingenfelter, S. Shankar, and M. H. Devoret, "Optimizing the nonlinearity and dissipation of a snail parametric amplifier for dynamic range," *Physical Review Applied*, Vol. 10, No. 5, 054020, 2018.

[44] Caves, C. M., "Quantum limits on noise in linear amplifiers," *Physical Review D*, Vol. 26, No. 8, 1817, 1982.

[45] Castellanos-Beltran, M. A., K. D. Irwin, G. C. Hilton, L. R. Vale, and K. W. Lehnert, "Amplification and squeezing of quantum noise with a tunable josephson metamaterial," *Nature Physics*, Vol. 4, No. 12, 929–931, 2008.

[46] Clerk, A. A., M. H. Devoret, S. M. Girvin, F. Marquardt, and R. J. Schoelkopf, "Introduction to quantum noise, measurement, and amplification," *Reviews of Modern Physics*, Vol. 82, No. 2, 1155–1208, 2010.

[47] Cullen, A. L., "Theory of the travelling-wave parametric amplifier," *Proceedings of The Iee-part B: Electronic and Communication Engineering*, Vol. 107, No. 32, 101–107, 1960.

[48] Naaman, O. and J. Aumentado, "Synthesis of parametrically coupled networks," *PRX Quantum*, Vol. 3, No. 2, 020201, 2022.

[49] Malnou, M. and J. Aumentado, "Deconstructing the traveling wave parametric amplifier," *IEEE Transactions on Microwave Theory and Techniques*, Vol. 72, No. 4, 2158–2167, 2024.

[50] Greco, A., L. Fasolo, A. Meda, L. Callegaro, and E. Enrico, "Quantum model for rf-squid-based metamaterials enabling three-wave mixing and four-wave mixing traveling-wave parametric amplification," *Physical Review B*, Vol. 104, No. 18, 184517, 2021.

[51] Macklin, C., K. O'brien, D. Hover, M. E. Schwartz, V. Bolkhovsky, X. Zhang, W. D. Oliver, and I. Siddiqi, "A near-quantum-limited josephson traveling-wave parametric amplifier," *Science*, Vol. 350, No. 6258, 307–310, 2015.

[52] Wustmann, W. and V. Shumeiko, "Parametric resonance in tunable superconducting cavities," *Physical Review B — Condensed Matter and Materials Physics*, Vol. 87, No. 18, 184501, 2013.

[53] Plenio, M. B. and S. F. Huelga, "Dephasing-assisted transport: Quantum networks and biomolecules," *New Journal of Physics*, Vol. 10, No. 11, 113019, 2008.

[54] Eichler, C., D. Bozyigit, C. Lang, M. Baur, L. Steffen, J. M. Fink, S. Filipp, and A. Wallraff, "Observation of two-mode squeezing in the microwave frequency domain," *Physical Review Letters*, Vol. 107, No. 11, 113601, 2011.

[55] Kraus, K., "General state changes in quantum theory," *Annals of Physics*, Vol. 64, No. 2, 311–335, 1971.

[56] Adesso, G. and F. Illuminati, "Entanglement in continuous-variable systems: recent advances and current perspectives," *Journal of Physics A: Mathematical and Theoretical*, Vol. 40, No. 28, 7821, 2007.

[57] Dolinar, S. J., "Optimum detection of coherent electromagnetic radiation," Ph.D. dissertation, Ph.D. dissertation, Stanford Univ., Stanford, CA, USA, 1973.

[58] Guha, S., "Quantum-enhanced sensing," *Phys. Rev. A*, Vol. 94, 012108, 2016.

[59] Shi, H., J. H. Shapiro, and Z. Zhang, "Practical quantum radar and lidar: physics, principles, and techniques," *J. Opt.*, Vol. 25, 013002, 2023.

[60] Reichert, L., A. Ferri, S. T. Johansen, C. Lupo, R. Elgharib, M. R. Vissers, L. Frunzio, M. H. Devoret, L. P. Pryadko, and A. A. Houck, "Quantum-enhanced sensing and readout of microwave resonators," *Phys. Rev. Res.*, Vol. 5, 023137, 2023.

[61] Skolnik, M. I., *Introduction to Radar Systems*, 2nd ed., McGraw-Hill, 1980.

[62] Luong, D. and B. Balaji, "Quantum radar with gaussian states and non-gaussian detectors: sensitivity and performance," *IEEE Trans. on Aerospace and Electronic Systems*, Vol. 58, 4239–4257, 2022.

[63] Mahafza, B. R., *Radar Systems Analysis and Design Using MATLAB*, 4th ed., CRC Press, 2022.

[64] Norouzi, M. and J. D. Saari, "Quantum radar: State of the art and new avenues," *IEEE Aerospace and Electronic Systems Magazine*, Vol. 38, 62–76, 2023.

[65] Barzanjeh, S., S. Pirandola, D. Vitali, and J. M. Fink, "Microwave quantum illumination using a digital receiver," *Science Advances*, Vol. 6, No. 19, eabb0451, 2020.

[66] Fasolo, L., C. Barone, M. Borghesi, G. Carapella, A. P. Caricato, I. Carusotto, W. Chung, A. Cian, D. D. Gioacchino, E. Enrico, *et al.*, "Bimodal approach for noise figures of merit evaluation in quantum-limited josephson traveling wave parametric amplifiers," *IEEE Transactions on Applied Superconductivity*, Vol. 32, No. 4, 1–6, 2022.